Dalton Transactions

Accepted Manuscript

ROYAL SOCIETY OF CHEMISTRY

www.rsc.org/dalton

Cite this: DOI: 10.1039/c0xx00000x

www.rsc.org/xxxxxx

ARTICLE TYPE

Asymmetric Hetero-assembly of Colloidal Nanoparticles through "Crash Reaction" in a Centrifugal Field

Sha Song,[a] Yun Kuang,[a] Liang Luo[a] and Xiaoming Sun*[a]

Received (in XXX, XXX) Xth XXXXXXXXX 20XX, Accepted Xth XXXXXXXXX 20XX

DOI: 10.1039/b000000x

Asymmetric hetero-assembly of two kinds of colloidal nanoparticles (NPs) was achieved by "crash reaction" in a density gradient centrifugation system using Au NPs as an example. Centrifugal force was applied to overcome Brown motion effect and cause NPs' directional movements. Water/oil interface was introduced to increase effective collision probability.

Assembly of nanoparticles (NPs) in a controlled scale is of great importance for exploiting their collective properties and bridging the gap between individual NPs and highly ordered nanostructures that are significant for fabrication of elaborate nanodevices. Previously, homo-aggregates such as dimers and trimers were prepared by exploiting either random aggregation,[1-3] steric effects[4-7] or specific control over surface ligands[8-11]. Compared with these homogeneous assemblies, heterogeneous assembly could link two or more kinds of distinct particles together.[12] It can not only combine properties associated with different kinds of particles, but also possibly show unique and superior properties, such as chemical and electronic anisotropy.

Fabrication of elaborate nanodevices requires precise control over size, morphology, stoichiometry, as well as symmetry. Centrosymmetric hetero-assembly could be achieved through spontaneously assembly of two kinds of NPs with different surface ligands. However, for asymmetric hetero-assembly, only templated assembly of NPs[13, 14] or synthesis of asymmetric particles[15-18] could achieve such symmetry control. Traditionally, colloidal hetero-assembly could only result in centrosymmetric assemblies because of random Brown motions of NPs, which greatly limited the availability of assembled particles and even hindered the applications of the assembled structures. Herein, we introduced a centrifugal field to the colloidal assembly system to overcome Brown motion effect and control the directional movements of NPs. Bigger NPs sediment faster than small NPs and thus "crashed reaction" would resulted in asymmetric hetero-assembly. Furthermore, when a water/oil interface was introduced to the density gradient, effective collision probability was greatly increased.

Fig. 1 schematically shows the "crash reaction" mechanism using Au NPs with different diameters as an example to illustrate the "crash reaction" concept. Firstly, hexadecyltrimethylammonium chloride (CTAC) stabilized 60nm and 20nm Au NPs were functionalized with positively charged ligand *p*-aminothiophenol (*p*-ATP) and negatively charged ligand 3-mercaptopropionic acid (MPA), respectively.[19] Then the two kinds of functionalized Au NPs were placed at different gradient layers. A buffer layer was used to avoid spontaneously assembly of the NPs with opposite charges.

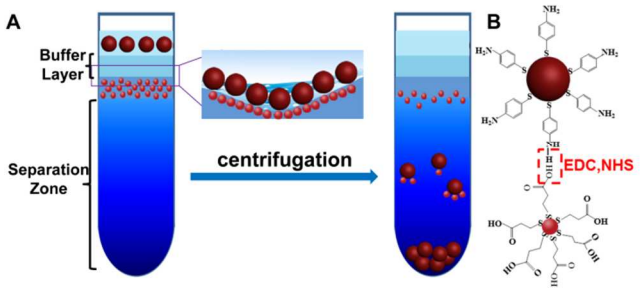

Fig. 1 (A) Schematic illustration of asymmetric hetero-assembly of different sized Au nanoparticles in a density gradient centrifugation system. (B) Functionalization of Au NPs and schematic linkage of NPs through EDC catalysed condensation of the amino and carboxyl groups.

According to the classical sedimentation theory,[20] the sedimentation velocity of spherical colloidal particles in a given medium with density ρ_s and viscosity η_s, in a centripetal field of g', can be described as

$$v = 2(\rho_p-\rho_s)\, r^2\, g'/(9\eta_s) \qquad \text{(I)}$$

where v is the sedimentation velocity of the nanoparticle, ρ_p and ρ_s are the densities of nanoparticle and surrounding fluid, r is the radius of the nanoparticle, g' is the centrifugal acceleration and η_s is the viscosity of the surrounding fluid. When centrifugal field was applied, since big NPs had larger radius and apparent density,[21] they would fall much faster than small ones according to the sedimentation equation (I), thus "crash" would happen when two kinds of NPs met.

However, whether two particles assembled into symmetric or asymmetric structures depended on the velocity difference between sedimentation and Brown motion. That is, if Brown motion played a dominant role, random assembly would lead to symmetric superstructure while only directional movement of NPs would bring about asymmetric assembly. According to Stokes-Einstein equation (II),[22] diffusion constant D of spherical nanoparticles could be calculated by:

$$D = k_B T/(6\pi r\eta_s) \qquad \text{(II)}$$

Where k_B is Boltzmann's constant and T is the absolute temperature. For nanoparticles with diameter of 60nm, the diffusion constant is calculated to be about 3.39μm^2/s (see Supporting Information for detail), which means that in one second, the 60nm particle is displaced about 1.84μm. However, the sedimentation velocity of 60nm nanoparticle is calculated to be 267μm/s at 10000RPM (about 17141g), which is much faster than Brown motion. Thus the motion trajectory of NPs was approximately linear along centrifugal tube axis, making "crash" possible. Meanwhile, such fast sedimentation velocity ensures that 60nm NPs quickly pass through the "crash" zone with only one side attached with 20nm NPs, guaranteeing asymmetric hetero-assembly. When two kinds of NPs collided together, electrostatic interaction firstly played a key role on assembly. Then EDC catalysed condensation of the amino and carboxyl groups further solidified the linkage of the collided NPs. The as assembled superstructures were then isolated from small NPs by consequent separation zone.

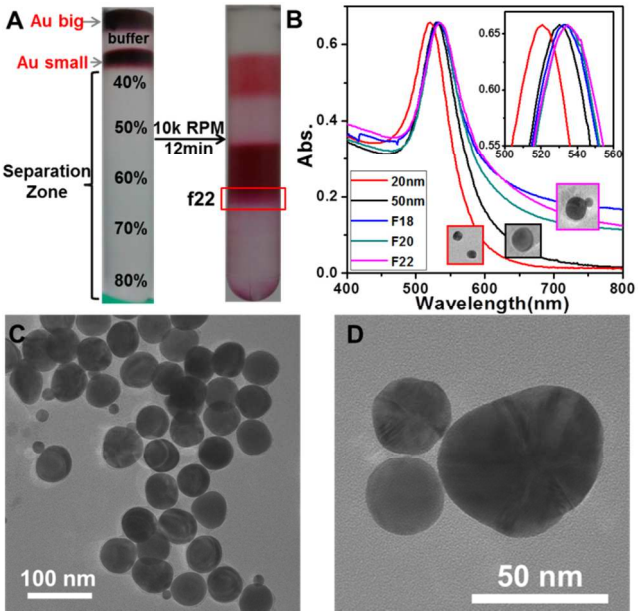

Fig. 2 (A) digital camera images of an 8 layer density gradient before and after "crash reaction", percentage represent volume content of ethylene glycol in water. (B) UV-Vis spectrums of 20nm, 60nm Au and fraction 18. (C) and (D) TEM images of the as assembled sample, f22.

Fig. 2A shows a typical "crash reaction" in an 8 layer density gradient. Highly concentrated 60nm Au nanoparticle solution was put on top of the gradient and 20 nm NPs were in 30% ethylene glycol (EG) solution layer. A buffer layer was placed between two Au NP layers to prevent spontaneously assembly of the NPs with opposite charges. When 17141g (10000RPM) centrifugal force was applied, the sedimentation velocities were calculated to be 267μm/s and 25μm/s for 60nm and 20nm NPs, respectively (see Supporting Information for detail). Therefore, 60nm NPs quickly passed through the buffer layer and reached reaction zone containing 20nm NPs and EDC-NHS catalysts. Then "crash reaction" happened when two kinds of particles met. Since the centrifugal force was quite great for particle sedimentation, 60nm NPs would quickly passed the reaction zone (less than 5s), avoiding random assembly of NPs with opposite charges. Finally, the assembled nanostructures fell into a 4-layer-gradient separation zone to separate the as-assembled superstructures from random aggregations. Fig. 2B shows UV-Vis spectrums of Au NPs before and after assembly. The plasmon extinction maxima of 20nm and 60nm NPs were found to be at 520 and 528nm, while fraction 18-22 showed little red shifts to 533 and 534nm, demonstrating assembly[19] of NPs and separation of the assemblies. TEM image (Fig. 2C) confirmed asymmetric assembly in fraction 22, though the proportion of the assemblies was quite low. It could be clearly seen that assembled NPs were linked tightly together (Fig. 2D). However, if the NPs with opposite charges were mixed without EDC catalysts, they would not tightly bond each other, as shown in Fig. S1. It should be mentioned that the "crash" probability was not quite high because the NPs were randomly isolated in solutions but not forming dense network, thus only a small ration of collision was effective collision.

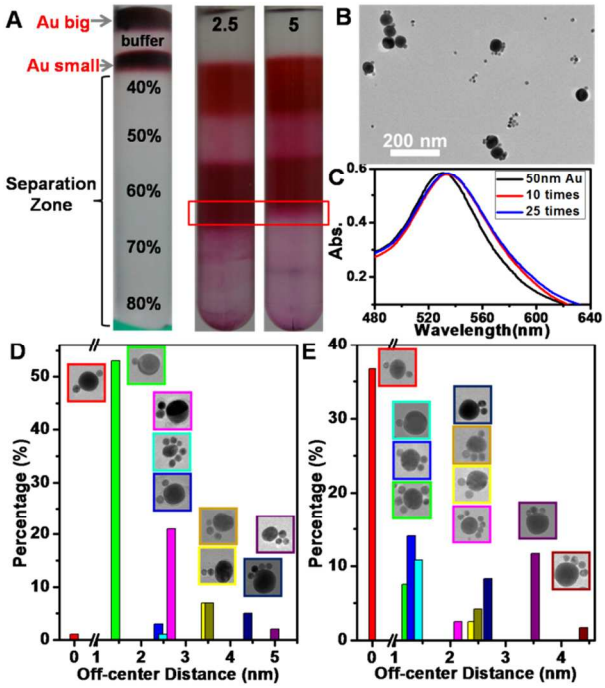

Fig. 3 (A) Digital camera image of tubes before and after centrifugation, the concentration of 20nm Au NPs was increased by 2.5 and 5 times. (B) TEM image of as assembled fraction for sample with 5 times concentration of 20nm Au NPs (C) UV-Vis spectrum of the fractions marked in red (D) Histogram of percentages of assemblies obtained from "crash reaction" vs. off-center distance(from gravity center to the center of big nanoparticle). (E) Histogram of percentages of assemblies obtained from random assembly vs. off-center distance(from gravity center to the center of big nanoparticle).

In order to increase the "crash" probability, we increased the concentration of small NPs by 2.5 and 5 times. TEM image clearly revealed increased amount of assemblies. The plasmon extinction maxima in UV-Vis spectrums also showed red shifts from 534nm (Fig.2C) to 535 and 536nm when the concentration of small NPs increased, demonstrating more assemblies contained. It should be mentioned that red shifts in UV-Vis spectrums are always very tiny for Au nanoparticles, 1nm shift in UV-Vis spectrum might because of tens of nanometres change in size.

We randomly selected 150 assembled particles from fraction 22 after "crash reaction" and 120 assembled particles from normal "random" crosslinking reaction to evaluate how much the small nanoparticles bind off-centered by analyzing their gravity center. We classified the TEM images, off-center distances (distance from the centre of big nanoparticle to the gravity centre of the assembly. See Fig. S2 for detail), numbers and percentages of different assembled structures in the table (Fig. S3 and Fig. S4) and showed the results as a histogram (Fig. 3D and Fig. 3E). It was shown that more than 95% hetero assemblies, which were obtained through "crash reaction" in a centrifugal field, were asymmetric hetero assemblies and most of the off-center distance located at 1.47 nm, 2.68 nm and 3.53 nm, representing typical assemblies of 1, 2 and 3 small particles linked to the same side of big nanoparticle. However, when we mixed these two types of particles in the same chemical environment for the same time period that "crash reaction" lasted, about 36.7% assemblies were almost symmetrical and 40% assemblies were random attaching of several small nanoparticle on a big nanoparticle core, while typical asymmetric hetero assemblies accounts for only 23.3%, which is much less than the percentage in "crash reaction" system. Therefore, such quantified data demonstrated asymmetric hetero assembly is taking place in "crash reaction" system.

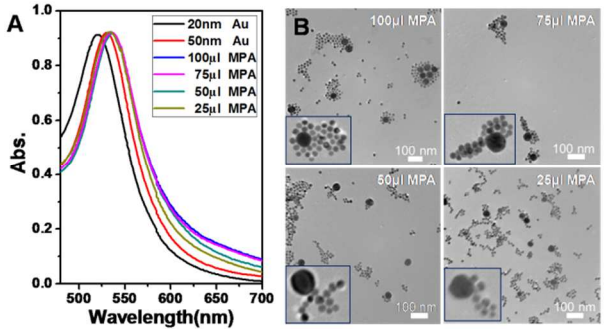

Fig. 4 (A) UV-Vis spectrums and (B) TEM images of as-assembled fraction with different amount of MPA (100µl, 75µl, 50µl and 25µl) used for functionalization of 20nm Au NPs.

Furthermore, the collision unit could be tuned by increasing the amount of MPA used for functionalization of 20nm Au NPs from 10µl to 25-100µl. As MPA was an acid with pKa ≈ 4.32, higher concentration resulted in higher ionic strength, which would lead to partial aggregation or homo-assembly of 20nm NPs, thus the collision unit could be changed from single small nanoparticle to small nanoparticle assembly, which means "denser" network for grabbing the "falling" big NPs. Fig. 4A shows UV-Vis spectrums of as-assembled fraction with different amount of MPA (100 µl, 75 µl, 50 µl and 25 µl) used for functionalization of 20 nm Au NPs. the red shift of plasmon extinction maxima revealed assembly of the superstructure, which was coincide with previous 10µl experiment shown in Fig. 2. Besides red shift of the extinction maxima, the right side of the peaks also showed little red shift, demonstrating different aggregation state of the NPs.[23-26] TEM images in Fig. 4B confirmed pre-aggregation of 20 nm Au NPs, it could be seen that both hetero-assemblies and colloidal 20nm Au NPs showed different aggregation state. It is interesting that altering MPA concentration could not only change the pre-aggregation state of 20 nm Au NPs but also regulating the assembly morphologies from Janus to comet-like or even tadpole-shaped hetero-assembly.

Further enhancement of the effective collision probability was carried out by introducing a water/oil interface to the density gradient (Fig. S5A). 35% CCl_4 solution in cyclohexane was layered between 20nm Au NP solution and 50% EG solution. This organic layer would prevent sedimentation of 20 nm Au nanoparticles when a low centrifugal force was applied to the system because of large interface tension. Therefore, 20 nm Au NPs would only accumulate at the interface to form a closed packed NP layer; however, such low centrifugal force would not hinder the sedimentation of 60 nm Au NPs. Therefore, 60 nm NPs firstly passed through the buffer layer and then collided the closely packed 20 nm NPs. Since the 20nm NPs are closely packed, nearly all the collision was effective collision. After "crash reaction", the assembled superstructures passed the water/oil interface through droplet sedimentation mechanism.[27] Fig. S5B shows the hetero-assembly of big and small Au NPs. The free small NPs were brought down by the droplets as they might occupy the gaps between the assembled superstructures when droplets formed.

The yield of asymmetric hetero-assemblies are relatively low, which is in contrast to our estimated collision probability of the two kinds of NPs (near 100%, see Supporting Information for detail), which means the "effective" collision probability was low. We attribute this phenomenon to the relatively weak electrostatic interactions between the two collided NPs and sluggish EDC catalysed amidation. Therefore, utilization of surface modification ligands containing more reactive groups might bring more asymmetric hetero-assemblies.

Conclusions

For the first time, density gradient ultracentrifugation was used for asymmetric hetero-assembly of two kinds of colloidal NPs by "crash reaction". Centrifugal force was applied to control the directional movements of NPs and overcome Brown motion effect. When water/oil interface was introduced to centrifugation system, effective collision probability was increased. This method paved a way to artificially manipulated asymmetric hetero-assembly of colloidal nanoparticles and will contribute to fabrication of elaborate nanodevices.

Acknowledgement

This work has been supported by National Natural Science Foundation of China and the 973 Program (2011CBA00503).

Notes and references

[a] *State Key Laboratory of Chemical Resource Engineering, Beijing University of Chemical Technology, P.O. Box 98, Beijing 100029, China Fax and Tel: 86-10-64448751; E-mail: sunxm@mail.buct.edu.cn*

† Electronic Supplementary Information (ESI) available: [Experimental details, supplementary figures, calculations of sedimentation velosities, Brown motion diffusion constant and collision probability]. See DOI: 10.1039/b000000x/

1. X. Wang, G. Li, T. Chen, M. Yang, Z. Zhang, T. Wu and H. Chen, *Nano Lett.*, 2008, **8**, 2643-2647.

2. W. Li, P. H. C. Camargo, X. Lu and Y. Xia, *Nano Lett.*, 2008, **9**, 485-490.
3. G. Chen, Y. Wang, M. Yang, J. Xu, S. J. Goh, M. Pan and H. Chen, *J. Am. Chem. Soc.*, 2010, **132**, 3644-3645.
4. J. H. Lee, D. P. Wernette, M. V. Yigit, J. Liu, Z. Wang and Y. Lu, *Angew.Chem. Int. Ed.*, 2007, **46**, 9006-9010.
5. L. C. Brousseau Iii, J. P. Novak, S. M. Marinakos and D. L. Feldheim, *Adv. Mater.*, 1999, **11**, 447-449.
6. T. Dadosh, Y. Gordin, R. Krahne, I. Khivrich, D. Mahalu, V. Frydman, J. Sperling, A. Yacoby and I. Bar-Joseph, *Nature*, 2005, **436**, 677-680.
7. T. Chen, M. Yang, X. Wang, L. H. Tan and H. Chen, *J. Am. Chem. Soc.*, 2008, **130**, 11858-11859.
8. G. A. DeVries, M. Brunnbauer, Y. Hu, A. M. Jackson, B. Long, B. T. Neltner, O. Uzun, B. H. Wunsch and F. Stellacci, *Science*, 2007, **315**, 358-361.
9. A. P. Alivisatos, K. P. Johnsson, X. Peng, T. E. Wilson, C. J. Loweth, M. P. Bruchez and P. G. Schultz, *Nature*, 1996, **382**, 609-611.
10. K.-M. Sung, D. W. Mosley, B. R. Peelle, S. Zhang and J. M. Jacobson, *J. Am. Chem. Soc.*, 2004, **126**, 5064-5065.
11. K. Nakata, Y. Hu, O. Uzun, O. Bakr and F. Stellacci, *Adv. Mater.*, 2008, **20**, 4294-4299.
12. Y. Wang, G. Chen, M. Yang, G. Silber, S. Xing, L. H. Tan, F. Wang, Y. Feng, X. Liu, S. Li and H. Chen, *Nat Commun*, 2010, **1**, 87.
13. Y. Yin, Y. Lu and Y. Xia, *J. Am. Chem. Soc.* , 2001, **123**, 771-772.
14. D. Wang and H. Möhwald, *J.Mater.Chem.* , 2004 **14**, 459–468.
15. D. Wang and Y. Li, *J. Am. Chem. Soc.*, 2010, **132**, 6280-6281.
16. L. Bai, Y. Kuang, J. Luo, D. G. Evans and X. Sun, *Chem. Commun.*, 2012, **48**, 6963-6965.
17. S. Sacanna, M. Korpics, K. Rodriguez, L. Colón-Meléndez, S.-H. Kim, D. J. Pine and G.-R. Yi, *Nat Commun*, 2013, **4**, 1688.
18. B. Liu, H. Möhwalda and D. Wang, *Chem. Commun.* , 2013, **49**, 9746-9748.
19. N. Gandra, A. Abbas, L. Tian and S. Singamaneni, *Nano Lett.*, 2012, **12**, 2645-2651.
20. C. A. Price, *Centrifugation in Density Gradients*, Academic Press, New York, 1982.
21. X. Sun, S. M. Tabakman, W.-S. Seo, L. Zhang, G. Zhang, S. Sherlock, L. Bai and H. Dai, *Angew. Chem. Int. Ed.*, 2009, **48**, 939-942.
22. A. Einstein, *Ann. Der. Physik*, 1905, **17**, 549-560.
23. F. Han, Z. Guan, T. S. Tan, and Q. Xu, ACS Appl. Mater. Interfaces 2012, **4**, 4746-4751.
24. M. Yang, G. Chen, Y. Zhao, G. Silber, Y. Wang, Sh-X. Xing, Y. Han and H. Chen, Phys. Chem. Chem. Phys., 2010, **12**, 11850-11860.
25. Y. Liu, X. Han, L. He and Y. Yin, *Angew. Chem. Int. Ed.* 2012, **51**, 6373-6377.
26. H. Zhang and D. Wang, *Angew. Chem. Int. Ed.* 2008, **120**, 4048-4051.
27. M. K. Brakke and J. M. Daly, *Science*, 1965, **148**, 387-389.